Implementation of Continuous 3D Whole Body PET Scanning Using On-the-fly Fourier Rebinning

Keishi Kitamura, Kazumi Tanaka, and Tomohiko Sato
Shimadzu Corporation, 1 Nishinokyo-kuwabara-cho, Nakagyo-ku, Kyoto, 604-8511 Japan

Abstract

Continuous scanning mode in 3D whole body PET studies has the advantage of axial sensitivity uniformity over the majority of the axial FOV. However this scan mode requires large data handling compared to conventional discrete scans. In this work, we have implemented and evaluated a new continuous 3D scan method using 'on-the-fly' Fourier rebinnig. In this method, sinograms for the pair of rings are added in real-time into the sinograms of the incremented ring pairs by moving the bed axially one detector width at a time. For a *N*-ring scanner, *2N-1* sinograms are transferred to a host computer at each bed position and rebinned into direct 2D sinograms using Fourier rebinning. Phantom and human studies showed that the axial image uniformity is achieved. This method can minimize the time for offline data processing and makes the continuous 3D scan more practical in clinical whole body studies.

I. INTRODUCTION

3D whole body PET scan offers the advantage of high sensitivity and can reduce patient dose while maintaining high signal to noise ratio (S/N). In conventional whole body scan, acquiring at distinct bed positions overlapping several slices results in an axially varying sensitivity profile due to the cylindrical geometry. In order to minimize the axial non-uniformity, it is necessary to optimize the number of overlapping end slices [1] and maximum ring differences being incorporated in the final images.

Several investigators have shown that the continuos axial sampling method is effective for the elimination of the axial S/N non-uniformity in the reconstructed images [2, 3, 4, 5]. This sampling method can be implement using conventional histogram mode acquisitions by moving the bed in a small discrete step or using list mode acquisitions by moving the bed in a true continuous motion. However, due to the vast amount of data produced by this scan mode, the total axial distance that can be covered is limited by the available memory and disk space. And the computation time for data to be re-sorted and added into sinograms may decrease the throughput of the continuous 3D scans.

In this work, we report on a new implementation of the 3D continuous scan mode using 'on-the-fly' Fourier rebinning, in which the bed is moved by axial width of detectors and synthesized sinogram data sets are transferred and rebinned into 2D sinograms at each bed position. This method does not require large memory and disk space and can improve data processing efficiency.

II. MATERIAL AND METHODS

A. Data Acquisition

All data were acquired on a Shimadzu SET-2400W PET scanner [6], which is a 32-ring system with an axial detector width of 6.25 mm and an axial FOV of 200 mm. In 3D mode, all possible coincidence pairs of 1024 sinograms are acquired. The front-end data acquisition system consists of large-scale acquisition memories (1GB) and a microprocessor that controls data collection in histogram mode, real-time corrections for dead time and decay of radioisotopes, and data transfer to a UNIX host computer with a storage disk. The acquisition software was modified for the continuous scan mode to move the bed by the axial width of detector, shift the memory address for sinogram matrices at each bed position, and write the data acquired to the disk sequentially, as described below.

For a *N*-ring scanner, N^2 sinograms $q_k(s, \phi, r_1, r_2)$ are acquired for the pair of rings (r_i, r_j) at the kth bed position. In the continuous scan mode, $q_k(s, \phi, r_1, r_2)$ are added into *2N-1* sinogram data set $p_h(s, \phi, \Delta r)$ in real-time as follows:

$$p_h(s, \phi, \Delta r) = \sum_{k=k_{\min}}^{k_{\max}} q_k(s, \phi, r_1 + k, r_2 + k) \qquad (1)$$

Where

$h = 0,1,2,\cdots,N + n - 1$,

$\Delta r = (r_1 - r_2) = 0, \pm 1, \pm 2, \cdots, \pm \Delta r_{\max}$,

$k_{\min} = \max\{0,\ h - n + 1\}$,

$k_{\max} = \min\{h,\ N - |\Delta r| - 1\}$.

In this work, we used $\Delta r_{\max} = N - 1$. With *n* bed positions, *N+n–1* data sets are acquired and each data set $p_h(s, \phi, \Delta r)$ consists of *2N-1* sinograms except for last *N-1* data sets. An example of the data sets is shown in Figure 1.

Lines of response (LOR's) corresponding to larger ring differences (larger azimuth angle) are measured less frequently than those with smaller ring differences. In general, LOR's with ring differences of Δr are measured N-$|\Delta r|$ times. In our implementation, the sets of ring difference data remain unscaled relative to each other. This means the sinograms being weighted by the number of times they are measured, which is able to improve S/N ratio in the final reconstructed image [3].

After the acquisition at the kth bed position, $p_h(s, \phi, \Delta r)$ is transferred to the host computer. After the data transfer is completed, the memory buffer can be reuse for a new data set. As a result, the total size of sinogram data sets for a 3D continuous scan is given by $(2N-1)\times(N+1)\times N_b$, not depending on the number of bed movements, where N_b is the number of bytes of memory buffer per sinogram.

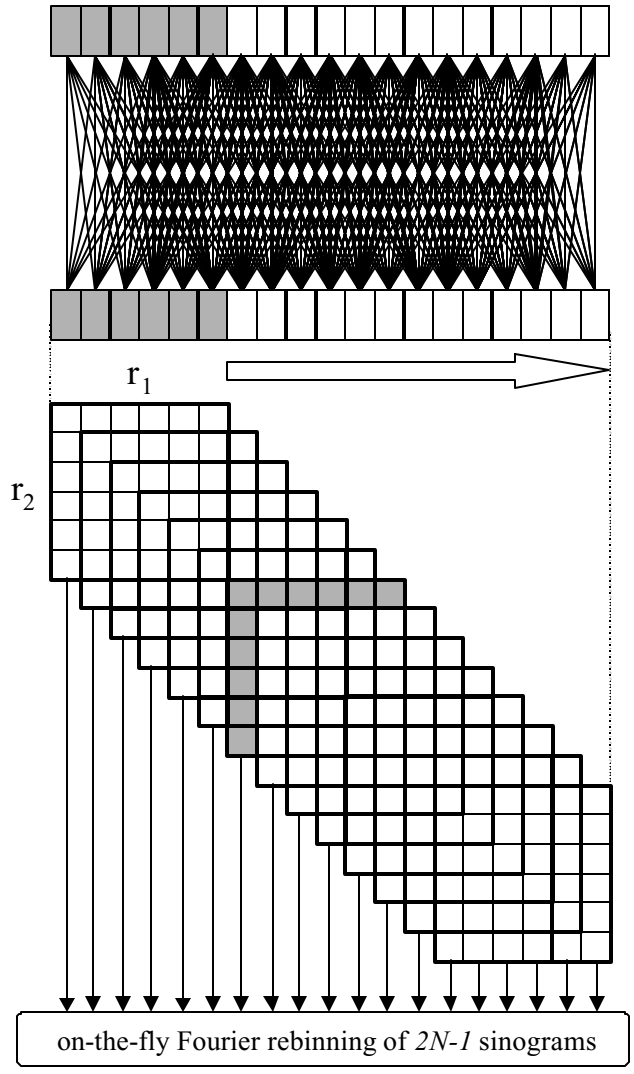

Fig. 1: Schematic representation of the lines of response and 3D data matrices for the continuous 3D whole body scan with a N = 6-ring scanner, which is indicated by the shaded detectors. In the 3D data space, each square corresponds to one oblique sinogram for the pair of rings (r_1, r_2), and each 6x6 matrix corresponds to sinogram data set at each bed position. The shaded area in the sinogram matrices is an example of synthesized sinogram data set, which is transferred and processed at each bed position.

B. Data Processing

To correct the transferred *2N-1* sinograms for detector efficiency variations, normalization correction factors are calculated from the conventional 3D normalization data by averaging normalize factors of the same ring differences in a similar way as (1). Attenuation correction factors are calculated from attenuation maps, which are reconstructed and assembled from 2D whole body transmission scans with conventional discrete bed motions.

The corrected sinograms are rebinned into 2D direct sinograms using Fourier rebinning [7]. In a given oblique sinogram, the azimuth angle is approximately constant, so a 1D interoperation across different oblique sinograms is not required. As a result, one data set transferred at each bed position can be processed independently, because it includes pairs of oblique sinograms with opposite values of Δr, which are merged to calculate discrete 2D Fourier transform as equation (6) in [7]. The resulting 2D data sets are reconstructed using 2D filtered backprojection or ordered subset EM (OSEM) algorithm [8].

C. Phantom and Human Studies

Phantom studies were performed in order to determine the axial uniformity in S/N using a 3D continuous data collection protocol compared with the conventional 3D whole-body scan protocol in the same total scan time. A 15cm diameter, 60 cm high cylindrical phantom containing about 2 mCi of F-18 were acquired. In the conventional discrete scans, data were acquired with 200 sec x 3 bed positions overlapping end slices of 5 or 10, and maximum ring difference of 22 was used for reconstruction. In the continuous scan, data were acquired with 10 sec x 60 bed positions. The percent standard deviation of the reconstructed images were calculated by drawing a 8 cm diameter ROI at the center of each image plane.

3D Whole body scans of a normal subject were also acquired in the conventional discrete scan and the continuous scan. In the discrete scan mode, emission data were acquired with 4 min x 3 bed positions overlapping 5 slices, 90 min after injection of 4 mCi ^{18}FDG. Transmission data were extracted from a 2D simultaneous emission and transmission scan acquired with 2 min x 3 bed positions. Attenuation correction factors were calculated from the reconstructed attenuation map processed with the non-linear Gausssian filters [9]. In the continuous scan mode, emission data were acquired with 12 sec x 60 bed positions. Emission images were in all cases reconstructed using OSEM reconstruction with 1 iteration and 24 subsets [6]. A post-reconstruction 2D Butterworth filter with 16 mm cut-off was applied to the images. No axial smoothing and weighted summation of overlapped images were performed.

III. RESULTS

Figure 2 shows the axial variation in standard deviation of the uniform cylinder for the discrete scan (solid line) with different overlap and for the continuous scan (circles). These

plots show that the continuous scan provide a better noise uniformity, while noise is amplified considerably near the gaps between bed positions in the discrete scan. Using 10 slice overlap, axial nonuniformity is slightly improved while the axial coverage is shortened.

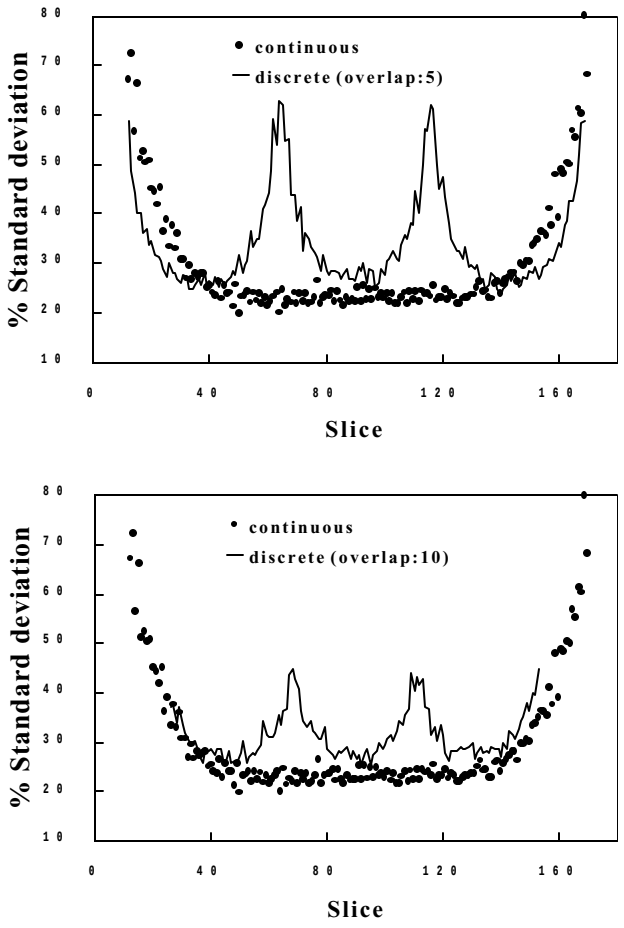

Fig. 2: Standard deviation/Mean of the 3D cylinder in a 10 cm diameter ROI placed at the center of the reconstructed image. The data were acquired using the discrete scan (solid lines) with overlapped slices of 5 (top) and 10 (bottom) and using the continuous scan (circles).

Figures 3 and 4 show coronal and sagittal cross sections from the normal subject scan using the conventional discrete scan (left) and the continuous scan (right). The images in the top rows have not been attenuation corrected and the images in the bottom rows have been attenuation corrected using the same attenuation map for the both scan modes.

As shown in these figures, in the discrete scan, there is an increase in noise and visual artifacts at the end of the slices of each axial FOV indicated by the arrows. In the continuous scan, these noise amplifications were eliminated and the spine appears much more clearly, indicating the overall improvement in S/N.

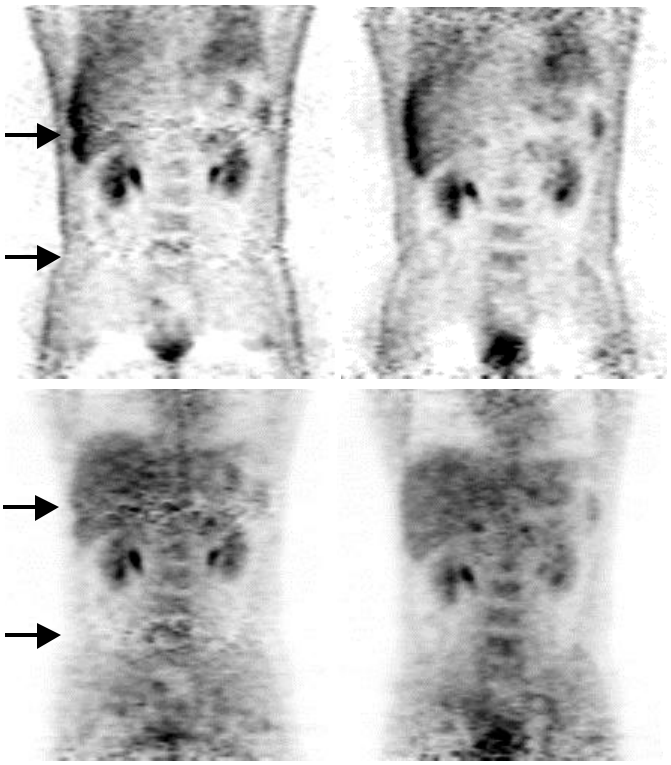

Fig. 3: Coronal cross sections through a normal subject using the discrete scan (left) and the continuous scan (right). The bottom images have been attenuation corrected.

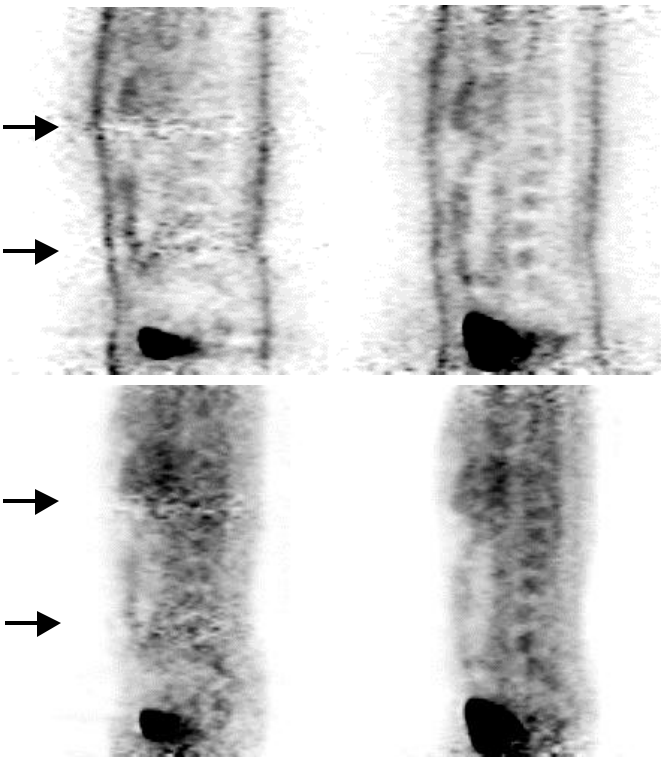

Fig. 4: Sagittal cross sections through a normal subject using the discrete scan (left) and the continuous scan (right). The bottom images have been attenuation corrected.

IV. DISCUSSION

The main advantage of the continuous scan is the axial S/N uniformity as shown in Fig. 2. In addition, the overall improvements in S/N of the whole body images can be seen in Fig. 3 and Fig. 4. In the continuous scan, all the data points in the central slices are sampled with all the detectors in the axial direction hence the detector efficiencies in the axial direction are averaged. As a result, S/N of the data corrected for detector efficiencies is slightly improved [10].

In this work, we have implemented continuous 3D whole body PET scanning using on-the-fly Fourier rebinning. This implementation has only required a slight modification to the acquisition software and a small size of acquisition memory and storage disk not depending on the axial coverage. Compared to the complete 3D data set, the size of sinogram data set that is transferred and processed at each bed position is small enough to be easy to handle. The program can be easily modified to improving axial sampling by decreasing the bed motion step and increasing the number of data set. But an axial sub-sampling is usually unnecessary in clinical whole body studies, because the axial resolution improvement is not significant [5].

The one drawback of the small step bed motion is that there is a dead time introduced between each bed motions. During the patient scan, it was found that this dead time loss is less than 8% of total acquisition time, which is not critical in clinical studies. It may be possible to modify the acquisition software for the microprocessor to move the bed in a true continuos motion and to be triggered at sampling time intervals to synthesize continuos sinograms.

V. SUMMARY

We have implemented the continuous scan for 3D whole body PET studies using the on-the-fly Fourier rebinning, in which sinograms are synthesized in the acquisition memory and transferred and processed after the acquisition at each bed position. Improved data processing efficiency can make the continuous 3D whole body scan more practical in routine clinical studies, while maintaining the axial S/N uniformity

VI. ACKNOWLEDGEMENTS

The authors wish to thank Mr. Masahiko Komatsu from Shimadzu SD Corporation for providing assistance in the implementation of the acquisition software, and staff of Yokohama City University Hospital for the acquisition of data.

VII. REFERENCES

[1] P. D. Cutler and M. Xu, “Strategies to improve 3D whole-body PET image reconstruction,” Phys. Med. Biol. vol.41, pp.1453-1467, 1996

[2] M. Dahlbom, D.-C. Yu, S. Cherry, A. Chatziioannou, and E. J. Hoffman, “Methods for improving image quality in whole body imaging,” IEEE Trans. Nucl. Sci., vol. NS-39, pp. 1079-1083, 1992.

[3] S. R. Cherry, M. Dahlbom, and E. J. Hoffman, “High sensitivity, total body PET scanning using 3D data acquisition and reconstruction,” IEEE Trans. Nucl. Sci., vol.39, no.4, pp.1088-1092, 1992

[4] M. Dahlbom, P. Cutler, W. Digby, P. Luk, and J. Reed, ”Characterization of sampling schemes for whole body PET imaging,” IEEE Trans. Nucl. Sci., vol. NS-41, pp. 1571-1576, 1994.

[5] M. Dahlbom, J. Reed, and J. Young, “Implementation of true continuous 2D/3D whole body PET Scanning,” Conference Record of the IEEE Nuclear Science Symposium and Medical Imaging Conference, Lyon, 2000

[6] T.Fujiwara, S Watanuki, S Yamamoto, M Miyake, S Seo, M Itho, K Ishii, H Orihara, H Fukuda, T Satoh, K Kitamura, K Tanaka, and S Takahashi, “Performance evaluation of a large axial field-of-view PET scanner:SET-2400W,” Annals of Nuclear Medicine, Vol.11, No.4, pp.307-313, 1997

[7] M. Defrise, P. E. Kinahan, and D. W. Townsend, “Exact and approximate rebinnig algorithm for 3-D PET data,” IEEE Trans. Med. Imag., vo.16, no.2, pp.145-157 ,1997

[8] H. M. Hudson and R. S. Larkin, “Accelerated image reconstruction using ordered subsets of projection data,” IEEE Trans. Med. Imag., vol. MI-13, pp. 601-609, 1994.

[9] K. Kitamura, H. Iida, M. Shidahara, S. Miura, and I. Kanno, “Noise reduction in PET attenuation correction using non-linear Gaussian filters,” IEEE Trans. Nucl. Sci., vol.47, no.3, pp.994-999, 2000

[10] A Chatziioannou and M Dahlbom, “Study on the effects of whole body PET spatial sampling schemes on data SNR", IEEE Nuclear Science Symposium and Medical Imaging Conference Record, pp. 1295-1299, vol.2, 1996